Nat Hazards (2012) 63:1157–1179
DOI 10.1007/s11069-012-0218-1

ORIGINAL PAPER

# A new approach to use AHP in landslide susceptibility mapping: a case study at Yenice (Karabuk, NW Turkey)

**Gökçe Deniz Hasekioğulları · Murat Ercanoglu**

Received: 22 February 2011 / Accepted: 8 May 2012 / Published online: 26 May 2012


**Abstract** This study aimed to investigate the parameter effects in preparing landslide susceptibility maps with a data-driven approach and to adapt this approach to analytical hierarchy process (AHP). For this purpose, at the first stage, landslide inventory of an area located in the Western Black Sea region of Turkey covering approximately 567 km$^2$ was prepared, and a total of 101 landslides were mapped. In order to assess the landslide susceptibility, a total of 13 parameters were considered as the input parameters: slope, aspect, plan curvature, topographical elevation, vegetation cover index, land use, distance to drainage, distance to roads, distance to structural elements, distance to ridges, stream power index, sediment transport capacity index, and wetness index. AHP was selected as the major assessment methodology since the adapted approach and AHP work in data pairs. Adapted to AHP, a similarity relation–based approach, namely landslide relation indicator (LRI) for parameter selection method, was also proposed. AHP and parametric effect analyses were performed by the proposed approach, and seven landslide susceptibility maps were produced. Among these maps, the best performance was gathered from the landslide susceptibility map produced by 9 parameter combinations using area under curve (AUC) approach. For this map, the AUC value was calculated as 0.797, while the others ranged between 0.686 and 0.771. According to this map, 38.3 % of the study area was classified as having very low, 8.5 % as low, 15.0 % as moderate, 20.3 % as high, and 17.9 % as very high landslide susceptibility, respectively. Based on the overall assessments, the proposed approach in this study was concluded as objective and applicable and yielded reasonable results.

**Keywords** Analytical hierarchy process · Landslide · Landslide susceptibility · Similarity relations · West Black Sea region

G. D. Hasekioğulları · M. Ercanoglu (✉)
Geological Engineering Department, Hacettepe University, 06800 Beytepe, Ankara, Turkey
e-mail: murate@hacettepe.edu.tr

## 1 Introduction

A natural disaster can be defined as some rapid, instantaneous, or profound impact of the natural environment upon the socio-economic system (Alexander 1993). In the last decades, there has been a dramatic increase in loss of lives and properties, as well as injuries and damages to the environment, as a result of natural disasters. In addition to increase in population, rapid and unconscious urbanization has also played an important role in these losses. Turkey, a country ranked among the most affected by natural disasters worldwide, has frequently witnessed the dreadful consequences of natural disasters such as earthquakes, landslides, floods, avalanches, and so on. Of these, landslides are the second destructive natural disaster in the country and constitute approximately 30 % of the whole damage. Therefore, it becomes necessary to assess landslides in order to mitigate landslide consequences by preparing landslide inventory, susceptibility, and hazard or risk maps. Landslide inventory and susceptibility maps, in particular, are of great importance since they provide important information for decision makers and planners and constitute the basic information for hazard and risk maps. In addition, effective utilization of these maps can considerably reduce damages and losses (Ercanoglu 2005). Although the hazard and risk concepts are very important, it is not usually possible to obtain required data for landslide hazard or risk assessment parameters. Thus, in this study, landslide susceptibility assessment is preferred in a landslide-prone area in Turkey.

Landslide susceptibility is defined as a quantitative or qualitative assessment of the classification, volume (or area), and spatial distribution of landslides that exist or potentially may occur in an area. Although it is expected that landsliding will occur more frequently in the most susceptible areas, in the susceptibility analysis, time frame is explicitly not taken into account (Fell et al. 2008). In other words, landslide susceptibility analysis involves developing an inventory of landslides that have occurred in the past together with an assessment of the frequency (annual probability) of the occurrence of landslides (Cascini 2008). In order to assess landslide susceptibility, there are qualitative and quantitative methods such as heuristic analysis (geomorphic analysis and qualitative map combination), knowledge-based analysis (based on a learning process), statistical analysis (discriminant analysis, factor analysis, logistic regression, and so on), and deterministic analysis (classical slope stability theory and factor of safety approach) (Soeters and Van Westen 1996; Fell et al. 2008). In a different study, Ayalew et al. (2005) categorized these methods into three groups such as semi-qualitative (simple ranking and rating and analytical hierarchy process), quantitative (bivariate, multivariate statistical analyses, neural networks and fuzzy approaches), and hybrid methods (index based and training based). To add another viewpoint, recent developments in geographic information system (GIS), remote sensing, and computer technologies allowed users to perform landslide susceptibility assessments in more feasible ways. Nowadays, practically all research on landslide susceptibility and hazard mapping makes use of digital tools for handling spatial data such as GIS, global positioning systems (GPS), and remote sensing (Van Westen et al. 2008). Thus, utilization of the quantitative methods has enormously increased and has become much more common than the qualitative ones. As for the landslide susceptibility assessment parameters (i.e., the causal or conditioning factors), users have a multitude of options to produce different input data layers based on geological, topographical, land use, and geomorphological features of the area concerned. Regardless of the assessment method, the input data for landslide susceptibility assessment should be selected on a basis of causes of actual and past instabilities. However, analysis of cause–effect relationship is not always simple, as a landslide is seldom linked to a single cause (Aleotti and Chowdhury 1999). Therefore, it becomes important to make a selection of the significant input parameters in landslide susceptibility assessments and modeling to obtain more reliable results. This selection depends usually upon experience, size of the area, time, scale, landslide type, methodology to be applied, project budget, data availability, and reliability (Glade and Crozier 2005). The crucial stage of this process is the selection of reliable data from what may be available (Aleotti and Chowdhury 1999).

In this study, taking into consideration the above-mentioned issues, the major objectives for selecting parameters and assessing landslide susceptibility were twofold: firstly, selecting or ordering the effects of input parameters on landslide occurrences and secondly, evaluating the landslide susceptibility by Analytical Hierarchy Process (AHP) based on the first stage. In order to achieve the first objective, the max–min (MM) method, one of the similarity methods in fuzzy logic (Ross 1995), was considered to represent the input parameter effects on landslide occurrences. A new index, namely landslide relation indicator (LRI), was proposed for the landslide susceptibility assessments. It depicts the parameter effect on landslide occurrences and allows users to order the parametric weights. In addition, the proposed index was adapted to AHP method. By doing so, it was thought that the subjectivity concept in AHP was alloyed by the proposed methodology in the present study.

## 2 Characteristics of the study area

The study area is located in the Western Black Sea region of Turkey (Fig. 1) and is known as one of the most landslide-prone areas in the country. It encompasses four 1/25,000 quadrangles and covers approximately 567 $km^2$, located in the west of Karabuk City. The digital elevation model (DEM) was obtained from the 1/25,000 scale topographical maps provided from the General Command of Mapping of Turkey. The DEM of the study area, containing 1418975 pixels with 20 m $\times$ 20 m resolution, represents that the topographical elevations range from 95 m to 1,736 m. Slope angle values vary between 0° and 59°. In the region, typical Black Sea climate prevails, and annual average rainfall is 518.2 mm (http://tumas.meteoroloji.gov.tr). The biggest residential location in the study area is the Yenice District of Karabuk City. There are also small scattered villages such as Döngeller, Kadıköy, Akmanlar, Keyfaller, and Güney. The main stream is the Yenice River, which passes through the study area approximately in its east–west direction. There are also Kelemen, Simsir, Pazarlı, and Güney Rivers, which form a dentritic drainage system in the study area.

There are eight different lithological units in the study area, ranging from Precambrian to Quaternary ages (Fig. 2). The oldest lithological units are metagranitoid, marble, and granite of Precambrian age. These units are covered by massive Jurassic limestones outcropped at highly steep slopes (Tuysuz et al. 2004). Jurassic limestones are overlaid by Lower Cretaceous conglomerates and sandstone–mudstone–limestone alternations. Upper Cretaceous age unit, known as Ulus formation, comprises of sandstone, claystone, and siltstone and represents turbiditic flysch character. This unit is very dominant in the Black Sea region, and its areal extent starts from south of Yenice and goes through in NW direction toward the Eastern Black Sea region. It is highly susceptible to weathering and has a weak structure. There is no landslide evidence in the resistant part of this unit (i.e., rock materials), while the non-resistant soil parts (i.e., weathering products of rocks) are highly prone to landslide occurrences, particularly in gentle slopes (Ercanoglu 2005). Quaternary alluvial deposits (Qal and Qy) are the youngest units and are generally

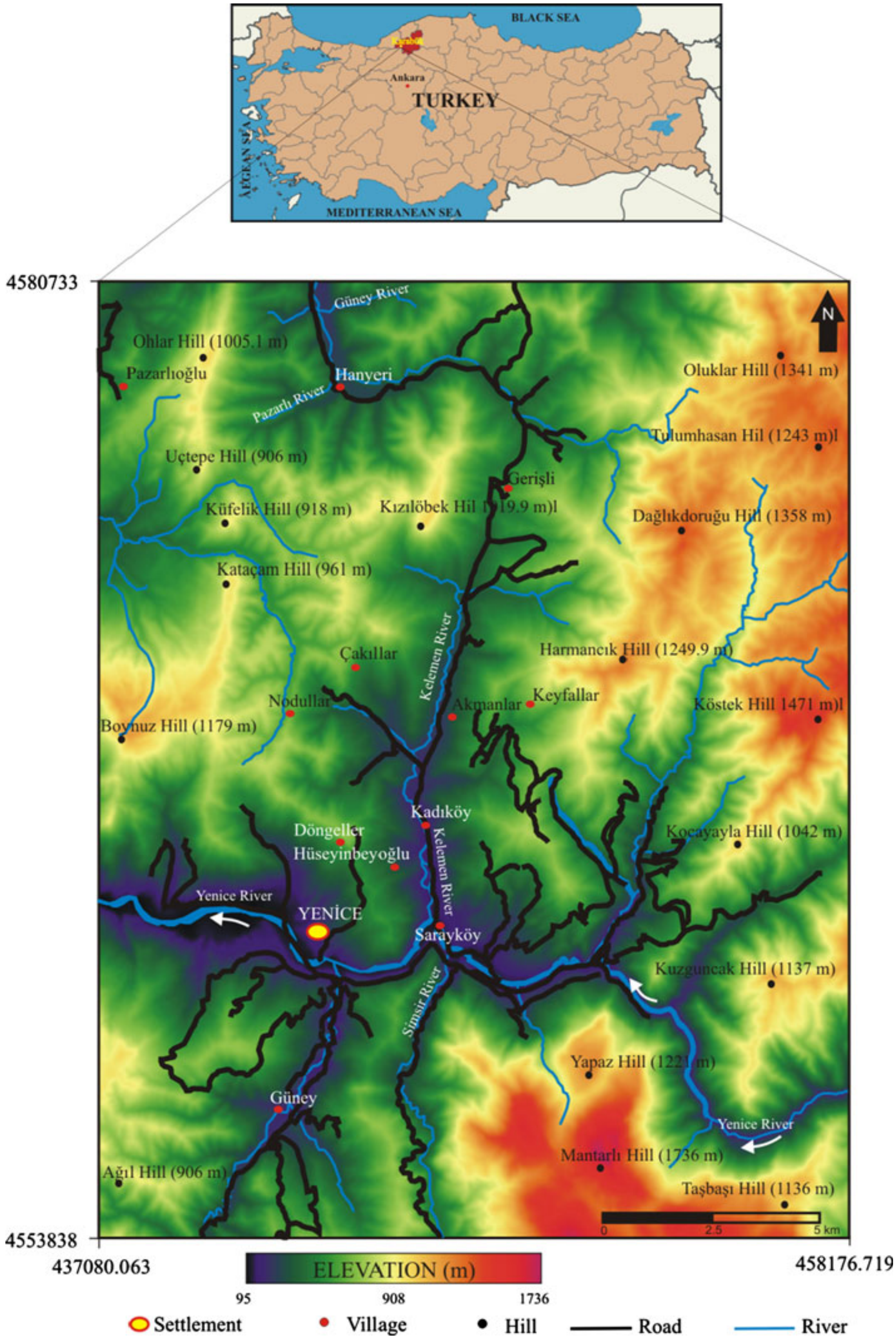


**Fig. 1** Location map of the study area

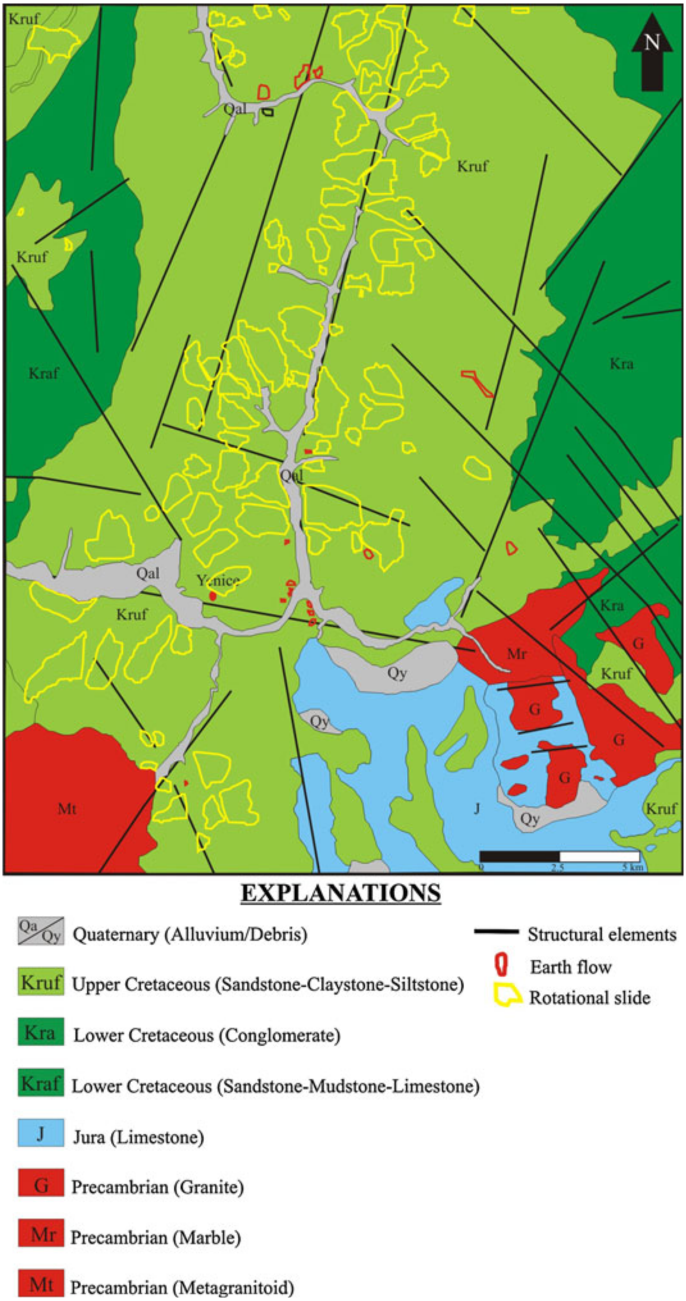


**Fig. 2** Geological map of the study area and mapped landslides

observed along the beds of the rivers and talus of slopes, respectively. Structural elements in the study area were obtained from the digital map prepared by MTA (2002) in vector format. However, no data exist regarding the type of structural elements in this map whether they are faults or folds.

To prepare landslide inventory map, at the first stage, landslide locations were determined by air photograph interpretations. Then, during the field studies, these locations were verified and mapped. In addition, landslide inventories of the previous works carried out in some parts of the study area (e.g., Ercanoglu and Gökçeoglu 2002; Ercanoglu et al. 2004; Can et al. 2005) were also confirmed and updated during the field studies to fulfill the actual landslide inventory. Totally, 101 landslide locations covering approximately 8.6 % of the study area were mapped based on these studies. Of these, 86 landslides were classified as rotational earth slides, while 15 landslides were classified as earth flow based on the landslide classification system proposed by Cruden and Varnes (1996) (Fig. 3). The largest landslide in the study area covers an area of 1.94 $km^2$, and the smallest one encompasses 7,655 $m^2$. Based on the information gathered from the local people, most of the landslides occurred after heavy rainfall and snowmelt events in different periods in the region. However, it was not possible to obtain much reliable data for each landslide from the records or people. But, it could be concluded that the main triggering factor of the landslide events was completely a result of the meteorological peaks.

## 3 Methodology

The first step in every landslide assessment includes the collection of available information and data related to the area concerned. Based on the purpose of mapping (i.e., susceptibility, hazard, or risk), these data can be subdivided into four groups such as landslide inventory data, environmental (causal) factors, triggering factors, and elements at risk (Van Westen et al. 2008). Of these, landslide inventory and environmental factors such as DEM, slope angle, aspect, lithology, land use, faults, and hydrological features are essential to landslide susceptibility mapping. However, there are no universal guidelines for selecting the parameters that influence landslides in susceptibility mapping (Ayalew et al. 2005). Thus, establishment of a link between causal parameters and landslides becomes a very important and a problematic issue.

The users have a lot of options to model landslide susceptibility, taking into consideration different data layers. The number of data layers in landslide susceptibility mapping may range from only a few parameters (e.g., Corominas et al. 2003; Moreiras 2005) to several parameters (Yesilnacar and Topal 2005 (17 parameters); Meusburger and Alewell 2008 (15 parameters)). A detailed study regarding the considered causal parameters in landslide susceptibility modeling was carried out by Hasekiogullari (2010). It was based on 114 scientific studies that were indexed in science citation index (SCI) and published in the period between 2000 and 2010 in different scientific journals. One of the major goals of that study was to evaluate the parametric preferences of the researchers when preparing landslide susceptibility maps. Based on the results of the study carried out by Hasekiogullari (2010), slope angle was the most commonly preferred causal parameter among the scientists. The other considered parameters and their utilization frequencies used in these studies are shown in Fig. 4. The question herein comes to mind why slope angle, lithology, aspect, topographical elevation, curvature, land use, and so on are much more preferred than the other parameters among the scientists. Of course, there is a theoretical background when selecting these parameters. For example, slope angle is the most important parameter in gravitational movements, while slope aspect might reflect differences in soil moisture and vegetation. Similarly, lithology controls the type of movement, and land-use/land-cover characteristics are one of the main components in stability analyses (Van Westen et al. 2008). In addition to the theoretical relationships with experience and data

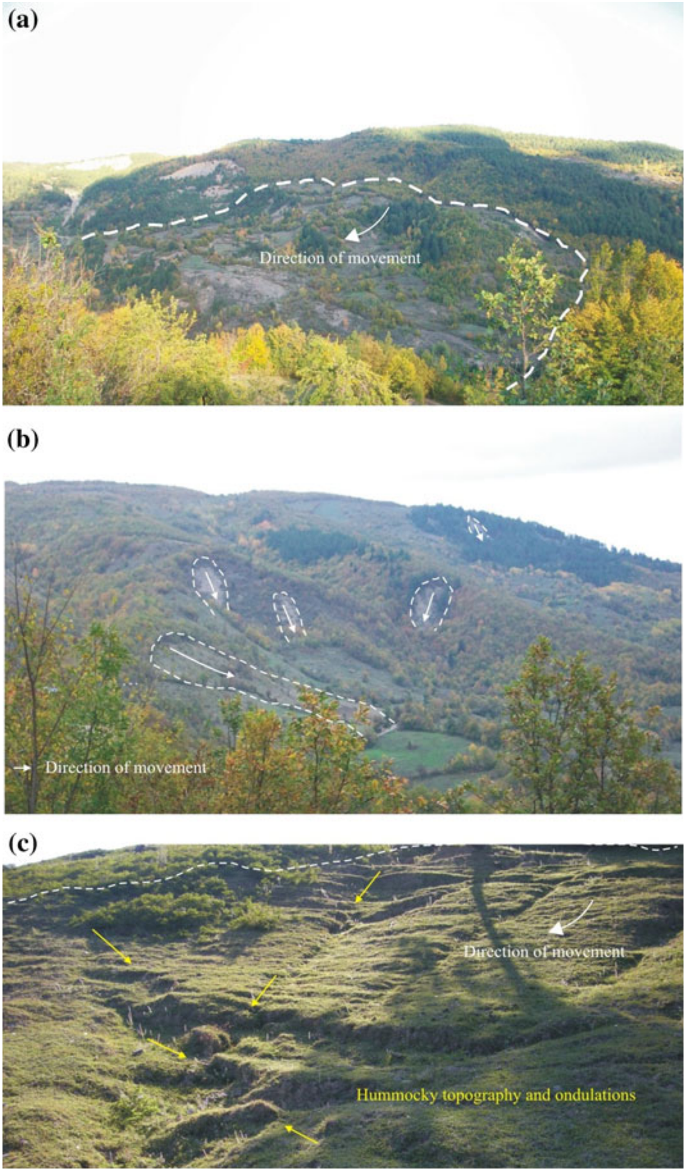


**Fig. 3** Some views from the landslides: **a** rotational slide; **b** earth flow; and **c** typical hummocky topography for rotational slides

availability, there are also technical reasons to use some other parameters. For example, if there is a module, let us say drainage density, in the GIS code used in a study, the user may want to use this feature as an input parameter in the landslide susceptibility analyses since the user may think a logical relationship between the drainage density and landslides. The development of a clear hierarchical methodology in landslide assessments is necessary to obtain an acceptable cost-benefit ratio and to ensure the practical applicability of the assessment (Soeters and Van Westen 1996). The scale parameter is also important for these studies and selecting landslide-related parameters. The working scale for a slope instability analysis is determined by the requirements of the user for whom the survey is executed. Although the selection of the scale of analysis is usually determined by the intended application of mapping results, the choice of a mapping technique remains open. This choice depends upon type of problem and availability of data, financial resources, and time for the investigation, as well as the professional experience of those involved in the survey (Soeters and Van Westen 1996). In this study, 1/25,000 scale maps such as topographical and land-use maps and their derivatives were used, based on the data at hand and data availability. Another aspect is that there are no fixed or standard value of weight and rating for landslide-related features. Furthermore, the determination of the weight and rating values are very important to landslide susceptibility analyses (Lee et al. 2004). This could be done by several methods such as statistical analyses (e.g., Ercanoglu et al. 2004; Ayalew and Yamagishi 2005; Guzzetti et al. 2008; Thiery et al. 2007; Nefeslioglu et al. 2008; Bai et al. 2009; Nandi and Shakoor 2009; Poudyal et al. 2010; Pradhan and Lee 2010), artificial intelligence techniques (e.g., Ercanoglu and Gökçeoglu 2002, 2004; Ercanoglu 2005; Ermini et al. 2005; Gomez and Kavzoglu 2005; Yesilnacar and Topal 2005; Kanungo et al. 2006; Pradhan et al. 2009; Yılmaz 2010), and expert opinion approaches (e.g., Barredo et al. 2000; Abella and Van Westen 2008; Ercanoglu et al. 2008; Ruff and Czurda 2008). The users have also a lot of options to produce landslide susceptibility maps using different methodologies such as artificial intelligence techniques (fuzzy logic, artificial neural networks, neurofuzzy), statistical methods (logistic regression, multivariate statistics, etc.), and combination and/or comparison of these methods. For example, some recent applications for artificial intelligence techniques can be found in Pradhan (2010a, 2011), Pradhan and Buchroithner (2010), Bui et al. (2011), Oh and Pradhan (2011), Sezer et al. (2011), and Akgun et al. (2012). For statistical applications and comparative studies, the details can be found in Yılmaz (2009, 2010), Pradhan (2010b, c), Pradhan and Pirasteh (2010), Pradhan et al. (2010a, b), Ercanoglu and Temiz (2011), and Akgun (2012).

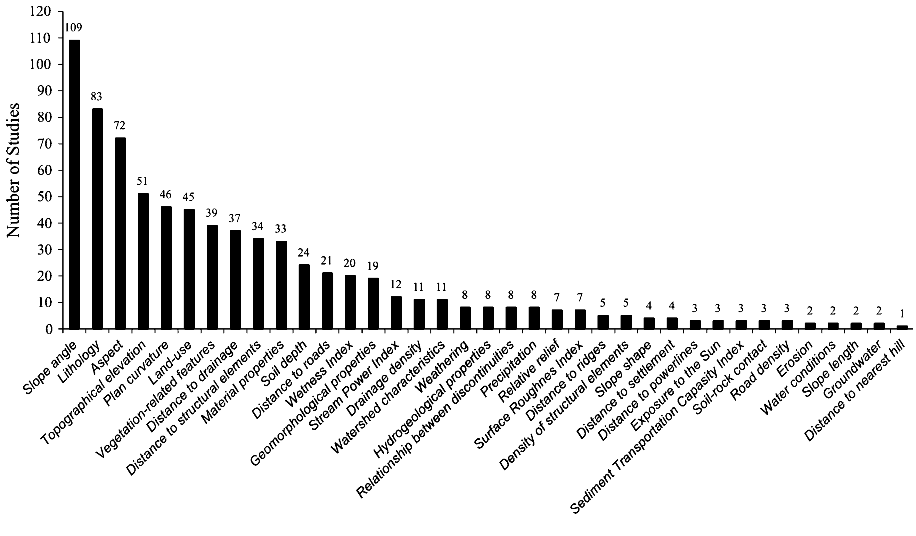


**Fig. 4** Distribution of the causal parameters considered in landslide susceptibility studies

This study attempted to evaluate landslide susceptibility by AHP, which can be considered in the expert opinion approaches. Generally, following steps are essential to perform AHP: (1) to break a complex unstructured problem down into its components; (2) to arrange the factors in a hierarchic order; (3) to assign numerical values to subjective judgment on the relative importance of each factor; and (4) to analyze the judgments to determine priorities to be assigned to these factors (Saaty and Vargas 2001). Perhaps, the most discussed step in this approach is the third step since it contains subjectivity with its general form. Although subjectivity is not necessarily bad when it is based on an expert opinion (Van Westen 2000), a new index, namely LRI, was adapted to overcome this problematic issue with this study. It is based on the "max–min" (MM) method, one of the similarity methods in fuzzy logic (Ross 1995). Similar to AHP, the MM method works on establishing relationships between elements of two or more data sets and operates on pairs of the data points. Although the name sounds similar to the fuzzy "max–min composition" method (Ercanoglu and Gökçeoglu 2004), it is different from the fuzzy composition operation. The MM method is expressed in the following equation:

$$r_{\mathrm{ij}} = \frac{\sum_{k=1}^{\mathrm{m}} \min(x_{\mathrm{ik}}, x_{\mathrm{jk}})}{\sum_{k=1}^{\mathrm{m}} \max(x_{\mathrm{ik}}, x_{\mathrm{jk}})} \quad i, j = 1, 2, \ldots, n \tag{1}$$

where $r_{\mathrm{ij}}$ is the similarity relation value, $x_{\mathrm{ik}}$ and $x_{\mathrm{jk}}$ are the members of the different data sets, and min and max are the minimum and the maximum values of the two data sets, respectively. Close values of $r_{\mathrm{ij}}$ to 1 indicate the similarity of the two data sets, while close values of $r_{\mathrm{ij}}$ to 0 show dissimilarity. The proposed LRI is based on the calculation of two different $r_{\mathrm{ij}}$ values, depicting the parameter effect on landslide occurrences by considering the parameters and landslide locations. It also allows users to order parameters based on the calculated LRI values, particularly for selecting the effective parameter combinations in the landslide susceptibility analyses. It is expressed in the following equation:

$$\mathrm{LRI} = \sum r_{\mathrm{ij(PR)}} \times r_{\mathrm{ij(LS)}} \tag{2}$$

where $r_{\mathrm{ij(PR)}}$ is the total calculated $r_{\mathrm{ij}}$ values of all the considered parameters with each other, $r_{\mathrm{ij(LS)}}$ is the $r_{\mathrm{ij}}$ value of any parameter with landslide locations, and LRI is the landslide relation indicator.

In order to calculate the LRI values for each parameter, 13 input parameter maps were prepared from different data sources (Table 1). As it is clear from Table 1, lithology parameter was not considered in the analyses. The main reason was that the mapped landslides were only located in the Upper Cretaceous flysch unit in the study area (see Fig. 2). Those parameters were almost compatible with the "top parameters" given in Fig. 4, frequently used in landslide susceptibility analyses. However, it should be noted that these parameters were gathered by the data availability and possibilities at hand in this study. Then, all vector-type parametric data were converted to raster files including the landslide inventory. Frequency ratio (FR) model proposed by Lee and Talib (2005) was used to associate these parameter maps with landslide locations. FR is the ratio of where landslides occurred in the total study area and also is the ratio of the probability of a landslide occurrence to a non-occurrence for a given attribute (Lee and Talib 2005). FR for each parameter was calculated in the GIS environment, considering randomly selected 70 % of overall data for modeling and 30 % for validation stages, respectively.

The calculated FR values were tabulated in Table 2. Also, these values were normalized (NFR) to express landslide susceptibility in [0, 1] interval, and the NFR values were assigned to the input parameter maps (Fig. 5). The next stage was to evaluate the LRI

**Table 1** Considered parameters in the analyses and their sources

| Parameter | Data source | Explanation |
|---|---|---|
| Land use | Ministry of Environment and Forestry of Turkey | Vector data |
| Distance to roads | Topographical maps | Digitized and stored in vector format |
| Normalized difference vegetation index | Landsat ETM+ | $\mathrm{NDVI} = \frac{\mathrm{IR}-\mathrm{R}}{\mathrm{IR}+\mathrm{R}}$, where IR is infrared band value; R is the red band value of the satellite image (Rouse et al. 1974) |
| Topographical elevation | General Command of Mapping of Turkey | Obtained in vector format and converted to DEM by interpolation |
| Slope angle | DEM | Derived from DEM |
| Distance to ridges | DEM | Derived from DEM using TauDEM (4.0) in vector format |
| Wetness index | DEM | $\mathrm{WIN} = \ln\left(\frac{\mathrm{As}}{\tan\beta}\right)$, where As is the specific catchment area, $\beta$ is the local slope (Beven and Kirkby 1979) |
| Plan curvature | DEM | Derived from DEM |
| Sediment transport capacity index | DEM | $\mathrm{STC} = (\mathrm{m}+1)\left(\mathrm{As}/_{22,3}\right)^{\mathrm{m}}\left(\sin\beta/_{0,896}\right)^{\mathrm{n}}$, where As is the specific catchment area, $\beta$ is the local slope, m and n values are 0.4 and 1.3, respectively (Moore and Wilson 1992) |
| Distance to streams | DEM | Derived from DEM using TauDEM (4.0) considering Strahler (1957) order greater than 5 in vector format |
| Aspect | DEM | Derived from DEM |
| Stream power index | DEM | $\mathrm{SPI} = \mathrm{As}.\ \tan\beta$, where As is the specific catchment area, $\beta$ is the local slope (Moore et al. 1991) |
| Distance to structural elements | MTA (2004) | Vector data |
| Landslide locations | Aerial photography + field mapping | Vector data |

**Table 2** Distribution of parameter subgroups in landslide locations and in the study area

| Parameter | LSA (%) | Grid (%) | FR | NFR |
|---|---|---|---|---|
| *Land use (LUS)* | | | | |
| Forest | 13.33 | 60.34 | 0.22 | 0.10 |
| Barren land | 2.89 | 1.42 | 2.04 | 0.93 |
| Water | 0.00 | 0.01 | 0.00 | 0.00 |
| Agriculture | 83.78 | 38.23 | 2.19 | 1.00 |
| *Aspect (ASP)* | | | | |
| Flat | 0.00 | 0.71 | 0.00 | 0.00 |
| N | 12.62 | 11.97 | 1.05 | 0.81 |
| NE | 13.45 | 12.84 | 1.05 | 0.81 |
| E | 13.13 | 12.16 | 1.08 | 0.83 |
| SE | 14.12 | 10.87 | 1.30 | 1.00 |
| S | 16.08 | 12.55 | 1.28 | 0.99 |
| SW | 13.03 | 13.72 | 0.95 | 0.73 |
| W | 9.94 | 13.90 | 0.71 | 0.55 |
| NW | 7.63 | 11.28 | 0.68 | 0.52 |
| *Plan curvature (PLC)* | | | | |
| PLC $\leq -2$ | 0.00 | 0.01 | 0.00 | 0.00 |
| $-2 <$ PLC $\leq -1$ | 0.60 | 1.04 | 0.58 | 0.52 |
| $-1 <$ PLC $\leq 0$ | 48.24 | 43.77 | 1.10 | 1.00 |
| $0 <$ PL $\leq 1$ | 50.93 | 54.49 | 0.93 | 0.85 |
| $1 <$ PLC $\leq 2$ | 0.22 | 0.69 | 0.31 | 0.28 |
| $2 <$ PLC | 0.00 | 0.02 | 0.00 | 0.00 |
| *Distance to stream(m) (DTS)* | | | | |
| DTS $\leq 250$ | 22.57 | 19.91 | 1.13 | 1.00 |
| $250 <$ DTS $\leq 500$ | 24.60 | 22.06 | 1.12 | 0.98 |
| $500 <$ DTS $\leq 750$ | 21.04 | 19.49 | 1.08 | 0.95 |
| $750 <$ DTS $\leq 1{,}000$ | 17.58 | 15.87 | 1.11 | 0.98 |
| $1{,}000 <$ DTS $\leq 1{,}250$ | 14.21 | 18.91 | 0.75 | 0.66 |
| $1{,}250 <$ DTS | 0.00 | 3.76 | 0.00 | 0.00 |
| *Normalized difference vegetation index (NDVI)* | | | | |
| NDVI $\leq -0.1$ | 0.00 | 0.04 | 0.00 | 0.00 |
| $-0.1 <$ NDVI $\leq 0$ | 0.06 | 0.16 | 0.37 | 0.18 |
| $0 <$ NDVI $\leq 0.1$ | 1.58 | 1.27 | 1.24 | 0.62 |
| $0.1 <$ NDVI $\leq 0.2$ | 9.05 | 4.87 | 1.86 | 0.93 |
| $0.2 <$ NDVI $\leq 0.3$ | 20.51 | 10.30 | 1.99 | 1.00 |
| $0.3 <$ NDVI $\leq 0.4$ | 24.84 | 13.29 | 1.87 | 0.94 |
| $0.4 <$ NDVI $\leq 0.5$ | 22.03 | 14.36 | 1.53 | 0.77 |
| $0.5 <$ NDVI $\leq 0.6$ | 15.09 | 25.44 | 0.59 | 0.30 |
| $0.6 <$ NDVI $\leq 0.7$ | 6.75 | 29.62 | 0.23 | 0.11 |
| $0.7 <$ NDVI | 0.09 | 0.65 | 0.13 | 0.07 |
| *Slope angle (°) (SLP)* | | | | |
| SLP $\leq 10$ | 5.22 | 8.42 | 0.62 | 0.46 |
| $10 <$ SLP $\leq 20$ | 60.34 | 44.92 | 1.34 | 1.00 |

**Table 2** continued

| Parameter | LSA (%) | Grid (%) | FR | NFR |
|---|---|---|---|---|
| $20 < \mathrm{SLP} \leq 30$ | 32.26 | 37.39 | 0.86 | 0.64 |
| $30 < \mathrm{SLP} \leq 40$ | 2.17 | 8.99 | 0.24 | 0.18 |
| $40 < \mathrm{SLP} \leq 50$ | 0.01 | 0.28 | 0.03 | 0.02 |
| $50 < \mathrm{SLP}$ | 0.00 | 0.00 | 0.00 | 0.00 |
| *Topographical elevation (m) (TEL)* | | | | |
| $\mathrm{TEL} \leq 250$ | 4.56 | 5.28 | 6.32 | 3.79 |
| $250 < \mathrm{TEL} \leq 500$ | 56.13 | 33.60 | 12.25 | 7.33 |
| $500 < \mathrm{TEL} \leq 750$ | 38.65 | 38.97 | 7.27 | 4.35 |
| $750 < \mathrm{TEL} \leq 1{,}000$ | 0.59 | 12.69 | 0.34 | 0.20 |
| $1{,}000 < \mathrm{TEL} \leq 1{,}250$ | 0.07 | 7.48 | 0.07 | 0.04 |
| $1{,}250 < \mathrm{TEL} \leq 1{,}500$ | 0.00 | 1.82 | 0.00 | 0.00 |
| $1{,}500 < \mathrm{TEL}$ | 0.00 | 0.16 | 0.00 | 0.00 |
| *Wetness index (WIN)* | | | | |
| $\mathrm{WIN} \leq 3$ | 0.00 | 0.00 | 0.00 | 0.00 |
| $3 < \mathrm{WIN} \leq 6$ | 36.71 | 52.90 | 0.69 | 0.48 |
| $6 < \mathrm{WIN} \leq 9$ | 56.89 | 42.55 | 1.34 | 0.92 |
| $9 < \mathrm{WIN} \leq 12$ | 5.74 | 3.93 | 1.46 | 1.00 |
| $12 < \mathrm{WIN}$ | 0.66 | 0.62 | 1.07 | 0.73 |
| *Stream power index (SPI)* | | | | |
| $0 \leq \mathrm{SPI} \leq 200$ | 49.91 | 58.93 | 0.85 | 0.50 |
| $200 < \mathrm{SPI} \leq 400$ | 40.57 | 34.39 | 1.18 | 0.70 |
| $400 < \mathrm{SPI} \leq 600$ | 7.20 | 4.56 | 1.58 | 0.94 |
| $600 < \mathrm{SPI} \leq 800$ | 2.32 | 1.38 | 1.68 | 1.00 |
| $800 < \mathrm{SPI}$ | 0.00 | 0.74 | 0.00 | 0.00 |
| *Sediment transport capacity index (STC)* | | | | |
| $0 \leq \mathrm{STC} \leq 25$ | 65.18 | 67.55 | 0.96 | 0.46 |
| $25 < \mathrm{STC} \leq 50$ | 24.96 | 23.75 | 1.05 | 0.50 |
| $50 < \mathrm{STC} \leq 100$ | 7.04 | 6.22 | 1.13 | 0.54 |
| $100 < \mathrm{STC} \leq 150$ | 2.82 | 1.34 | 2.11 | 1.00 |
| $150 < \mathrm{STC}$ | 0.00 | 1.14 | 0.00 | 0.00 |
| *Distance to ridges (m) (DTRI)* | | | | |
| $0 < \mathrm{DTRI} \leq 500$ | 95.11 | 94.84 | 1.00 | 0.92 |
| $500 < \mathrm{DTRI} \leq 1000$ | 4.71 | 4.35 | 1.08 | 1.00 |
| $1{,}000 < \mathrm{DTRI} \leq 1{,}500$ | 0.18 | 0.70 | 0.25 | 0.23 |
| $1{,}500 < \mathrm{DTRI}$ | 0.00 | 0.11 | 0.00 | 0.00 |
| *Distance to roads (m) (DTR)* | | | | |
| $0 < \mathrm{DTR} \leq 250$ | 32.04 | 22.04 | 1.45 | 0.88 |
| $250 < \mathrm{DTR} \leq 500$ | 26.88 | 16.28 | 1.65 | 1.00 |
| $500 < \mathrm{DTR} \leq 750$ | 18.44 | 11.71 | 1.57 | 0.95 |
| $750 < \mathrm{DTR} \leq 1{,}000$ | 11.56 | 8.69 | 1.33 | 0.81 |
| $1{,}000 < \mathrm{DTR} \leq 1{,}250$ | 11.08 | 31.23 | 0.35 | 0.21 |
| $1{,}250 < \mathrm{DTR}$ | 0.00 | 10.05 | 0.00 | 0.00 |

**Table 2** continued

| Parameter | LSA (%) | Grid (%) | FR | NFR |
|---|---|---|---|---|
| *Distance to structural elements (m) (DSE)* | | | | |
| $0 < \text{DSE} \leq 250$ | 11.74 | 18.33 | 0.64 | 0.30 |
| $250 < \text{DSE} \leq 500$ | 17.19 | 19.03 | 0.90 | 0.42 |
| $500 < \text{DSE} \leq 750$ | 17.90 | 17.28 | 1.04 | 0.48 |
| $750 < \text{DSE} \leq 1{,}000$ | 17.79 | 14.57 | 1.22 | 0.56 |
| $1{,}000 < \text{DSE} \leq 1{,}250$ | 35.38 | 16.35 | 2.16 | 1.00 |
| $1{,}250 < \text{DSE}$ | 0.00 | 14.44 | 0.00 | 0.00 |

*LSA* landslide-affected grid percentage; Grid (%) percentage of grids in domain, *FR* frequency ratio, *NFR* normalized frequency ratio

values of the input parameters. Thus, all input parameter and landslide inventory maps (including 0 for non-landslide and 1 for landslide locations) were converted to the data files ("*.dat"). To perform these analyses and to calculate LRI values for each parameter, a computer code, "LRI. bas", was written using the Q-Basic programming language. The work-flow diagram was given in Fig. 6. In order to calculate LRI value, two $r_{ij}$ values such as $r_{ij(PR)}$ and $r_{ij(LS)}$ are needed, as stated in Eq. 2. The first one (i.e., $r_{ij(PR)}$) defines the landslide susceptibility relationship between the parameter pairs, while the second one (i.e., $r_{ij(LS)}$) reflects the relationship between the considered parameter and landslide locations. This was needed because of the fact that two parameters could be compatible with each other but could not be consistent with the landslide locations, or vice versa. Thus, $r_{ij(PR)}$ and $r_{ij(LS)}$ values were calculated separately using "LRI.bas" and are given in Table 3. As can be seen from Table 3, the highest LRI value was obtained from slope angle (SLP) parameter as 2.716, and its order was the first. This means that the slope angle (SLP) and distance to streams (DTS) are the first two effective parameters on landslide occurrences in the study area, while the distance to ridges (DTRI) parameter has the lowest effect based on the LRI values. Thus, evaluation of the relative importance of the considered parameters with respect to the LRI values allowed selecting in which order the considered parameters contributed to landslide occurrences objectively.

In order to produce landslide susceptibility maps, AHP method was chosen since it considers parameter pairs similar to the LRI approach explained above. It is a multicriteria decision-making process using the relative importance of the parameters contributing to the event to produce parameter weights and evaluates the consistency of pairwise comparison parameter (Barredo et al. 2000). To date, AHP was successfully applied in many studies (e.g., Ayalew et al. 2005; Komac 2006; Yalçin and Bulut 2007; Akgün et al. 2008; Ercanoglu et al. 2008; Yalçin 2008; Wang et al. 2009; Akgün and Türk 2010; Huang et al. 2010). Generally, an expert rates the considered parameters based on a scale proposed by Saaty (1977) (Table 4). Pairwise importance of the parameters for an event is assessed by an expert, based on the values given in Table 4. These values are placed in an "n × n" matrix (n: the number of parameters) in the form of rows-to-columns order. To perform AHP analyses, WEIGHT and Multi-Criteria/Multi-Objective Decision Wizard (MCE) modules of Idrisi Taiga were used. The first module develops a set of relative weights for a group of parameters in a multicriteria evaluation. The weights generated by this module are produced by means of the principal eigenvector of the pairwise comparison matrix (Eastman 2009). This module also calculates the consistency ratio (CR), which shows the considered weights consistent or not. CR values less than 0.1 indicate a good consistency,

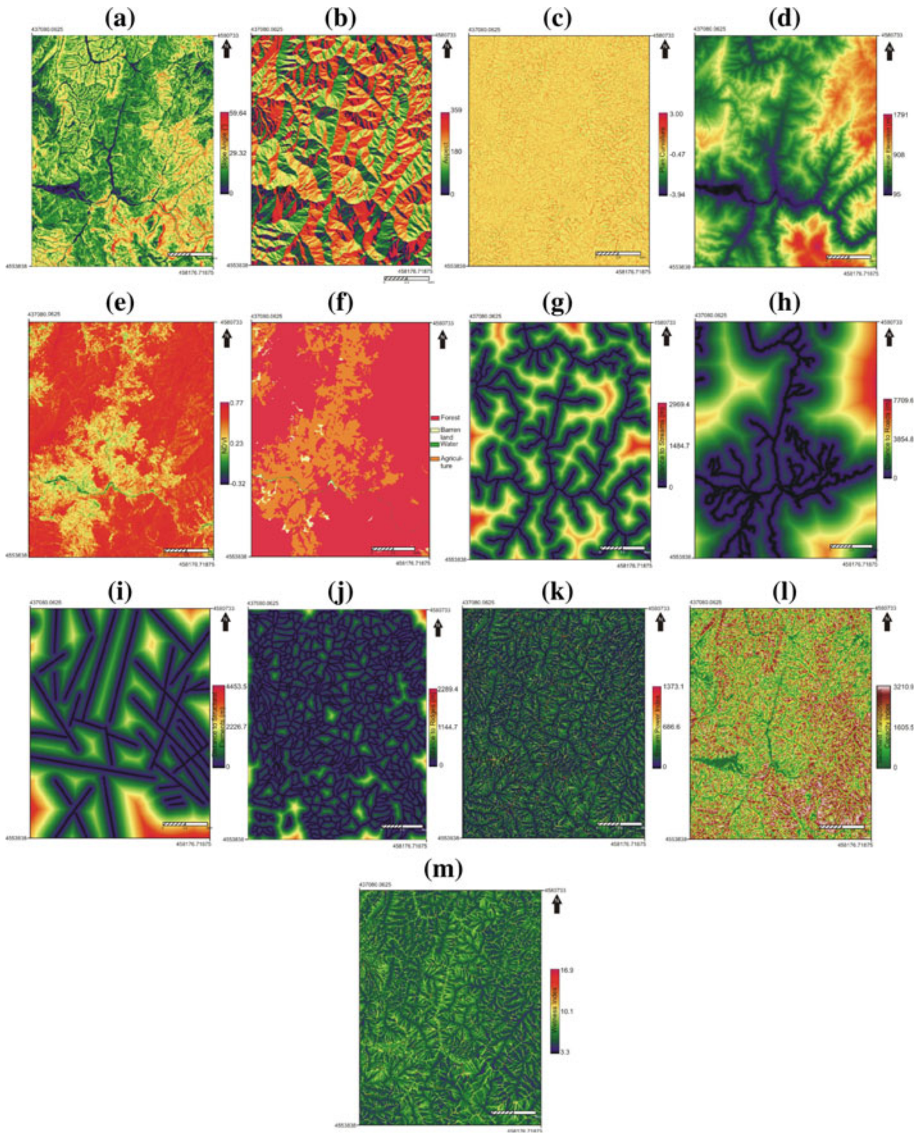


**Fig. 5** Considered input parameters: **a** slope; **b** aspect; **c** plan curvature; **d** topographical elevation; **e** NDVI; **f** land use; **g** distance to streams; **h** distance to roads; **i** distance to structural elements; **j** distance to ridges; **k** stream power index; **l** sediment transport capacity index; and **m** wetness index

while CR value exceeding 0.1 shows an inconsistent matrix and should be reevaluated. The MCE module provides a process in which multiple layers are aggregated to yield a single output map. It has three different procedures such as Boolean intersection, order weighted average (OWA), and weighted linear combination (WLC). Of these, the WLC was chosen to produce landslide susceptibility maps. It is a procedure of multiplying each factor by its factor weight and adding the results (Eastman 2009).

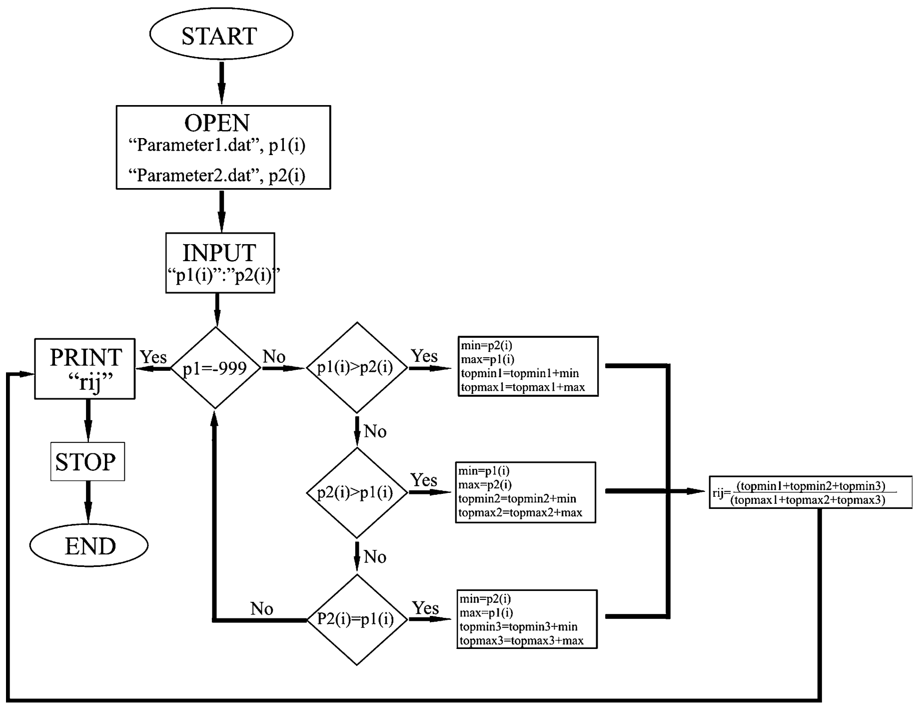


**Fig. 6** Flowchart of the "LRI.bas" computer code

**Table 3** LRI, $r_{ij(PR)}$, and $r_{ij(LS)}$ values of the considered parameters

| Parameter | $\sum r_{ij}$ (PR) | $r_{ij}$ (LS) | LRI | Order |
|---|---|---|---|---|
| Land use | 6.061 | 0.266 | 1.612 | 9 |
| Distance to roads | 7.491 | 0.143 | 1.071 | 12 |
| NDVI | 9.143 | 0.232 | 2.121 | 3 |
| Topographical elevation | 7.402 | 0.248 | 1.836 | 4 |
| Slope angle | 9.914 | 0.274 | 2.716 | 1 |
| Distance to ridges | 6.963 | 0.087 | 0.606 | 13 |
| Wetness index | 8.131 | 0.199 | 1.618 | 8 |
| Plan curvature | 8.122 | 0.212 | 1.722 | 5 |
| Sediment transport capacity index | 7.196 | 0.157 | 1.129 | 11 |
| Distance to streams | 8.112 | 0.269 | 2.182 | 2 |
| Aspect | 8.152 | 0.209 | 1.663 | 6 |
| Stream power index | 7.992 | 0.205 | 1.638 | 7 |
| Distance to structural elements | 7.351 | 0.165 | 1.213 | 10 |

In this study, instead of using an expert opinion to fulfill the parametric pairwise matrices, we made use of the calculated $r_{ij(PR)}$ and LRI values. This procedure allowed using a data-driven approach when assigning the parametric pairwise values. In order to achieve this, $r_{ij(PR)}$ values ranging in [0, 1] interval were adapted to the scale provided by Saaty (1977) (Table 5). The main idea herein is to build a logical connection between

**Table 4** Scale of relative importance between parameter pairs suggested by Saaty (1977)

| Intensity of importance | Definition | Explanation |
|---|---|---|
| 1 | Equal importance | Two activities contribute equally to objective |
| 3 | Weak importance of one over another | Experience and judgment slightly favor one activity over another |
| 5 | Essential or strong importance | Experience and judgment strongly favor one activity over another |
| 7 | Demonstrated importance | An activity is strongly favored and its dominance demonstrated in practice |
| 9 | Absolute importance | The evidence favoring one activity over another is the highest possible order of affirmation |
| 2, 4, 6, 8 | Intermediate values between the two adjacent judgments | When compromise is needed |

**Table 5** $r_{ij(PR)}$ values corresponding the relative importance values in AHP

| $r_{ij(PR)}$ | Intensity of importance[a] | Intensity of importance[b] |
|---|---|---|
| $0 \leq r_{ij(PR)} \leq 0.2$ | 9 | 1/9 |
| $0.2 < r_{ij(PR)} \leq 0.3$ | 8 | 1/8 |
| $0.3 < r_{ij(PR)} \leq 0.4$ | 7 | 1/7 |
| $0.4 < r_{ij(PR)} \leq 0.5$ | 6 | 1/6 |
| $0.5 < r_{ij(PR)} \leq 0.6$ | 5 | 1/5 |
| $0.6 < r_{ij(PR)} \leq 0.7$ | 4 | 1/4 |
| $0.7 < r_{ij(PR)} \leq 0.8$ | 3 | 1/3 |
| $0.8 < r_{ij(PR)} \leq 0.9$ | 2 | 1/2 |
| $0.9 < r_{ij(PR)} \leq 1.0$ | 1 | 1 |

[a] If the $r_{ij(LS)\text{Parameter1}} > r_{ij(LS)\text{Parameter2}}$

[b] If the $r_{ij(LS)\text{Parameter1}} < r_{ij(LS)\text{Parameter2}}$

$r_{ij(PR)}$ and relative importance values. This is realized by considering the relationship between the two parameter pairs with low $r_{ij(PR)}$ values (e.g., $0 \leq r_{ij(PR)} \leq 0.2$) should have the highest intensity of importance (e.g., 9 or 1/9 in the AHP scale) since one of the parameters dominates the landslide process and has absolute effect on landslide occurrence than the other one. Similarly, if the two parameters have almost the same effect (i.e., together contributing or not) on landslide occurrence or non-occurrence, $r_{ij(PR)}$ value between the two parameters must be high and has almost equal importance on the event (e.g., 1 in the AHP scale).

Given the above-mentioned issues, intensity of importance values among the parameter pairs were filled out in the matrices with the corresponding $r_{ij(PR)}$ values in Table 5. An example of a completed matrix with nine input parameters (selected by the orders given in Table 3) is given in Table 6. It should be noted that the intensity of importance values may be fractional or integer (ranging from 1/9 to 9) based on the location of parameter either in row or in column. For example, if the $r_{ij(PR)}$ value was calculated as 0.725 between the SLP and ASP parameters, the intensity of importance value would be 3 or 1/3 based on the values tabulated in Table 5. In this condition, the user could make a decision according to the LRI values of the considered parameters ($LRI_{SLP}$: 2.716; $LRI_{ASP}$: 1.663). If the SLP is in the row location and the ASP is in the column location (as in the case in Table 6), the importance value will be 3 since the SLP has higher effect on landslide occurrence due to

**Table 6** Comparison matrix for the nine parameters

| | LUS | ASP | PLC | DTS | NDVI | SLP | TEL | WIN | SPI |
|---|---|---|---|---|---|---|---|---|---|
| LUS | 1 | | | | | | | | |
| ASP | 1/2 | 1 | | | | | | | |
| PLC | 1/2 | 1 | 1 | | | | | | |
| DTS | 3 | 3 | 3 | 1 | | | | | |
| NDVI | 1/2 | 4 | 2 | 1/2 | 1 | | | | |
| SLP | 4 | 3 | 4 | 2 | 3 | 1 | | | |
| TEL | 1/2 | 2 | 2 | 1/3 | 1/2 | 1/3 | 1 | | |
| WIN | 1/2 | 2 | 1 | 1/2 | 1/2 | 1/4 | 1/2 | 1 | |
| SPI | 1/3 | 1/2 | 1/2 | 1/3 | 1/2 | 1/4 | 1/2 | 1 | 1 |

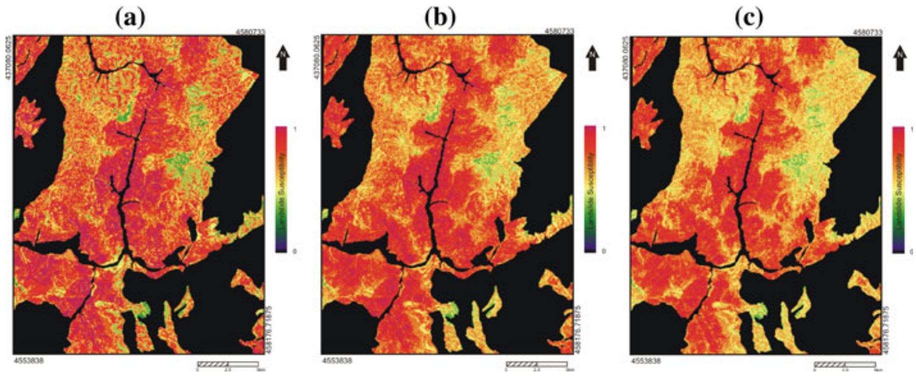


**Fig. 7** Landslide susceptibility maps produced by: **a** 3 parameters; **b** 6 parameters; and **c** 9 parameters

its higher LRI value. In contrast, if the ASP had been located in the row and the SLP had been located in the column of the matrix, the importance value would have been 1/3 (reciprocal value in the matrix) because of $LRI_{SLP}$: 2.716 > $LRI_{ASP}$: 1.663. Eventually, taking into consideration these assignments, a total of 11 matrices starting from first 3 parameters (SLP, DTS, and NDVI) with the highest LRI values to 13 parameter combinations (i.e., all parameters) were prepared. In other words, there were 11 different landslide susceptibility maps to be produced. Of these, three landslide susceptibility maps were shown in Fig. 7 in order to save space. Based on the CR values, except for 4 parameter combinations of 10, 11, 12, and 13, the CR values of 3–9 parameter combinations were obtained below 0.1. In other words, the parameter combinations ranging from 3 to 9 indicated the compatibility, while the others were not acceptable because of their CR values (Fig. 8). Thus, the maps produced by 10–13 parameters were not taken into consideration for the validation process. In addition, calculated weights for each parameter combinations were also shown in Fig. 8.

## 4 Results and validation

In the present study, landslide susceptibility was assessed in a landslide-prone area covering approximately 567 $km^2$ in the Western Black Sea region of Turkey. A total of 101

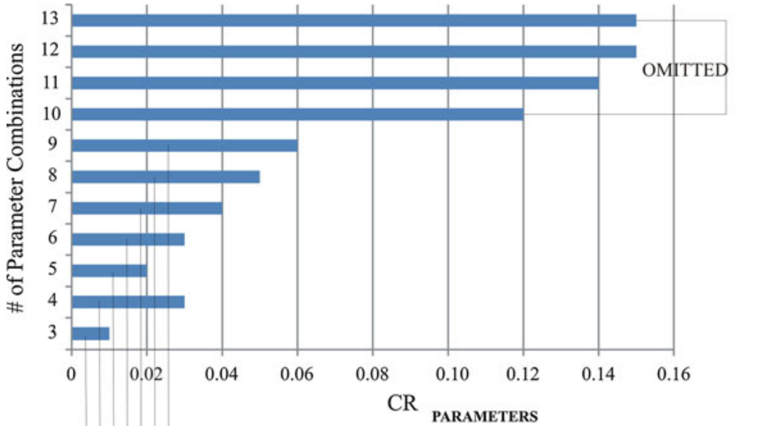


| SLP | DTS | NDVI | TEL | PLC | ASP | SPI | WIN | LUS |
|---|---|---|---|---|---|---|---|---|
| 0.519 | 0.297 | 0.184 | — | — | — | — | — | — |
| 0.427 | 0.283 | 0.164 | 0.126 | — | — | — | — | — |
| 0.395 | 0.261 | 0.155 | 0.111 | 0.078 | — | — | — | — |
| 0.345 | 0.240 | 0.167 | 0.107 | 0.072 | 0.069 | — | — | — |
| 0.313 | 0.214 | 0.156 | 0.106 | 0.075 | 0.074 | 0.062 | — | — |
| 0.289 | 0.190 | 0.144 | 0.104 | 0.071 | 0.071 | 0.066 | 0.065 | — |
| 0.275 | 0.178 | 0.131 | 0.088 | 0.074 | 0.073 | 0.068 | 0.057 | 0.056 |

**Fig. 8** CR values' parametric weights of the AHP models

landslides were mapped in the study area. In order to assess landslide susceptibility, basically, AHP model was considered. As mentioned before, 13 different parameter maps were used to produce landslide susceptibility maps. A total of 11 landslide susceptibility maps were produced for the study area using different parameter combinations, based on LRI concept and AHP. Of these, four landslide susceptibility maps were omitted because of the limitation related to CR values explained in the previous chapter. For these susceptibility maps, different susceptibility levels were obtained. In order to express spatial distribution or variability of landslide susceptibility, there are several ways such as quantiles, natural breaks, equal intervals, and standard deviations (Ayalew and Yamagishi 2005; Pradhan and Lee 2010). In this study, equal area division approach was followed to represent spatial variations in landslide susceptibility values varying from "very low" to "very high", dividing the [0, 1] interval by five classes with a unit of 0.2 increment. For all considered landslide susceptibility maps, spatial distributions of susceptibility levels are given in Table 7.

In order to validate the produced landslide susceptibility maps, Relative Operating Characteristics (ROC) module of Idrisi Taiga was applied using the validation data. This module evaluates the validity of a model that predicts the location of the occurrence of a class by comparing a suitability image depicting the likelihood of that class (i.e., the input image) and a Boolean image showing where that class actually exists (i.e., the reference image) (Eastman 2009). The module calculates the area under curve (AUC) value with the defined threshold (selected as 100 in the analyses). The value of 1 indicates that there is a perfect spatial agreement between the reference image and the input image, while the value of 0.5 is the agreement that would be expected due to chance. The ROC module also produces the true-positive (TP) % and false-positive (FP) % values for each threshold that constitute the curve from which the AUC is calculated. Based on the module results

**Table 7** Areal coverages of landslide susceptibility for the maps and AUC values of the AHP models

| AHP models | Areal coverages of landslide susceptibility levels (%) | | | | | AUC (%) |
|---|---|---|---|---|---|---|
| | Very low | Low | Moderate | High | Very high | |
| 3 Parameters | 37.5 | 1.7 | 10.6 | 25.9 | 24.3 | 68.6 |
| 4 Parameters | 38.0 | 2.1 | 11.3 | 25.6 | 23.0 | 70.2 |
| 5 Parameters | 38.1 | 3.7 | 19.9 | 26.0 | 12.3 | 71.9 |
| 6 Parameters | 38.4 | 2.6 | 7.4 | 28.9 | 22.7 | 73.4 |
| 7 Parameters | 38.2 | 2.5 | 8.0 | 31.2 | 20.1 | 75.3 |
| 8 Parameters | 39.2 | 9.7 | 15.4 | 17.0 | 18.7 | 77.1 |
| 9 Parameters | 38.3 | 8.5 | 15.0 | 20.3 | 17.9 | 79.7 |

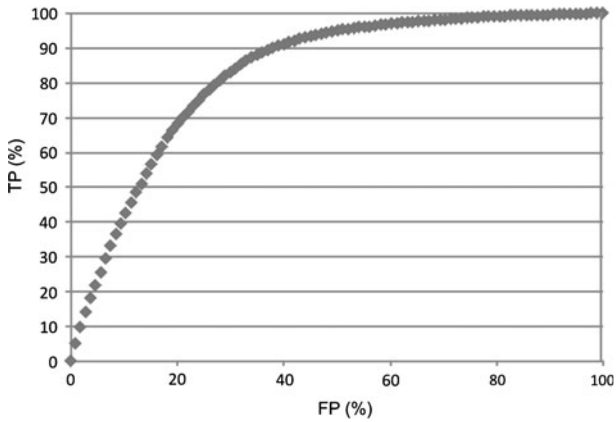


**Fig. 9** Performance of the landslide susceptibility map produced by 9 parameters

(Table 7), the best performance was gathered from the 9-parameter-combination landslide susceptibility map with the AUC value of 79.7 % (Fig. 9) using the validation data.

## 5 Conclusions and discussion

AHP model is conventionally based on a rating system provided by expert opinion. In fact, expert opinion is very useful in solving complex problems like landslides. However, to some extent, opinions may change for every individual expert and thus may be subjected to cognitive limitations with uncertainty and subjectivity. Another aspect is that data-driven methods are also powerful in landslide susceptibility mapping and contain less subjectivity. In order to minimize these drawbacks both in selecting parameters and in applying methodology, LRI, a new index, was proposed in this study. The LRI is applicable in any landslide susceptibility assessment method and allows users to order parametric importance before the landslide susceptibility analyses application. It is based on two similarity relation values depicting parametric relationships (by parametric pairwises) on landslide occurrences and landslide locations individually (by each parameter and landslide locations). The first one defines the landslide susceptibility relationships between the parameter pairs, while the second one reflects the relationship between the parameters and landslide locations. The main idea in the proposed approach is to reflect the parameter effects on landslide occurrences, considering the landslide system as a whole. In other words, two considered parameters could be compatible with each other on landslide locations but could not be consistent with landslide locations, or vice versa. For example, LUS (land use) parameter has the ninth order with respect to LRI values in the whole system. However, it is in the third order if only the landslide locations were considered. This means that LUS parameter is compatible with the mapped landslide locations, while it is not in accordance with the other parameters contributing the landslide system since most of the landslides occur only in agricultural lands (83.78 % of the landslide locations). Based on the LRI calculations, the parameter effects on landslide occurrences in order were the slope angle, distance to streams, NDVI, topographical elevation, plan curvature, aspect, stream power index, wetness index, land use, distance to structural elements, sediment transport capacity index, distance to roads, and distance to ridges, respectively. Taking into consideration this parametric order, different parameter combinations ranging from 3 to 13, a total of 11 AHP assessments were performed. Based on the CR values, 7 landslide susceptibility maps were produced since CR values of 10-11-12-13 parameter combinations were greater than 0.1. Of these, landslide susceptibility map produced by 9 parameter combinations showed the best performance with AUC value of 0.797 and was considered as satisfactory.

The difficulty in obtaining data and the issue of selecting independent data to analyze, that is, the parameters that are thought to be causally related, remain challenges in implementing more data-based approaches (Akgun 2012). Although the AHP method is fundamentally based on expert opinion, it is thought that the selection of parameters on landslide occurrences by LRI approach alloys the subjectivity concept in this method. Furthermore, LRI approach can be used in any landslide susceptibility assessment whatever the methodology is conducted. However, it should be noted that the reliability of the results is directly affected by the landslide location data, that is, the landslide inventory map. Research results will be helpful in developing new regulations on territory protection and facilities as well as land management purposes for local administrations, decision makers, and planners.

**Acknowledgments** This research is supported by the Scientific and Technical Research Council of Turkey (TUBITAK) (Project No: 108Y034). The authors would like to thank the Editor and two anonymous reviewers for their valuable comments and suggestions, which highly increased the quality of the paper. The authors would also like to thank Ms. Sibel Doğanay for her kind help and suggestions in English editing process.

## References

Abella EAC, Van Westen CJ (2008) Qualitative landslide susceptibility assessment bymulticriteria analysis: a case study from San Antonio del Sur, Guantánamo, Cuba. Geomorphology 94:453–466

Akgun A (2012) A comparison of landslide susceptibility maps produced by logistic regression, multi-criteria decision, and likelihood ratio methods: a case study at İzmir, Turkey. Landslides 9:93–106

Akgün A, Türk N (2010) Landslide susceptibility mapping for Ayvalik (Western Turkey) and its vicinity by multicriteria decision analysis. Environ Earth Sci 61:595–611

Akgün A, Sezer EA, Nefeslioglu HA, Gokceoglu C, Pradhan B (2012) An easy-to-use MATLAB program (MamLand) for the assessment of landslide susceptibility using a Mamdani fuzzy algorithm. Comp Geosci 38(1):23–34

Akgün A, Dağ S, Bulut F (2008) Landslide susceptibility mapping for a landslide-prone area (Findikli, NE of Turkey) by likelihood-frequency ratio and weighted linear combination models. Environ Geol 54:1127–1143

Aleotti P, Chowdhury R (1999) Landslide hazard assessment: summary review and new perspectives. Bull Eng Geol Environ 58:1–44

Alexander D (1993) Natural disasters. UCL Press, London

Ayalew L, Yamagishi H (2005) The application of GIS-based logistic regression for landslide susceptibility mapping in the Kakuda-Yahiko Mountains, Central Japan. Geomorphology 65:15–31

Ayalew L, Yamagishi H, Marui H, Kanno T (2005) Landslides in Sado Island of Japan: Part II. GIS-based susceptibility mapping with comparisons of results from two methods and verifications. Eng Geol 81:432–445

Bai SB, Wang J, Lü GN, Zhou PG, Hou SS, Xu SN (2009) GIS-based and data-driven bivariate landslide-susceptibility mapping in the three gorges area, China. Pedosphere 19(1):14–20

Barredo JI, Benavides A, Hervas J, Van Westen CJ (2000) Comparing heuristic landslide hazard assessment techniques using GIS in the Trijana basin, Gran Canaria Island, Spain. JAG 2(1):9–23

Beven KJ, Kirkby MJ (1979) A physically based, variable contributing area model of basin hydrology. Hydrol Sci Bull 24:43–69

Bui DT, Pradhan B, Lofman O, Revhaug I, Dick OB (2011) Landslide susceptibility mapping at Hoa Binh province (Vietnam) using an adaptive neuro fuzzy inference system and GIS. Comp Geosci. doi:10.1016/j.cageo.2011.10.031

Can T, Nefeslioglu HA, Gökçeoğlu C, Sönmez H, Duman TY (2005) Susceptibility assessments of shallow earthflows triggered by heavy rainfall at three catchments by logistic regression analyses. Geomorphology 72:250–271

Cascini L (2008) Applicability of landslide susceptibility and hazard zoning at different scales. Eng Geol 102:164–167

Corominas J, Copons R, Vilaplana JM, Altimir J, Amigó J (2003) Integrated landslide susceptibility analysis and hazard assessment in the principality of Andorra. Nat Haz 30:421–435

Cruden DM, Varnes DJ (1996) Landslide types and processes. In: Turner AK, Schuster RL (eds) Landslides: investigation and mitigation. Transportation research board, Special report 247. National Academy Press, Washington, pp 36–75

Eastman JR (2009) Idrisi Taiga, guide to GIS and image processing, user's guide (Ver. 15). Clark University Press, USA, 328 pp

Ercanoglu M (2005) Landslide susceptibility assessment of SE Bartin (West Black Sea region, Turkey) by artificial neural networks. Nat Haz Earth Sys Sci 5:979–992

Ercanoglu M, Gökçeoğlu C (2002) Assessment of landslide susceptibility for a landslide-prone area (north of Yenice, NW Turkey) by fuzzy approach. Env Geol 41:720–730

Ercanoglu M, Gökçeoğlu C (2004) Use of fuzzy relations to produce landslide susceptibility map of a landslide prone area (West Black Sea Region, Turkey). Eng Geol 75:229–250

Ercanoglu M, Temiz FA (2011) Application of logistic regression and fuzzy operators to landslide susceptibility assessment in Azdavay (Kastamonu, Turkey). Environ Earth Sci 64:949–964

Ercanoglu M, Gökçeoğlu C, Van Asch ThWJ (2004) Landslide susceptibility zoning north of Yenice (NW Turkey) by multivariate statistical techniques. Nat Haz 32:1–23

Ercanoglu M, Kaşmer Ö, Temiz N (2008) Adaptation and comparison of expert opinion to analytical hierarchy process for landslide susceptibility mapping. Bull Eng Geol Environ 67:565–578

Ermini L, Catani F, Casagli N (2005) Artificial neural networks applied to landslide susceptibility assessment. Geomorphology 66:327–343

Fell R, Corominas J, Bonnard C, Cascini L, Leroi E, Savage WZ (2008) Guidelines for landslide susceptibility, hazard and risk zoning for land use planning. Eng Geol 102:85–98

Glade T, Crozier MJ (2005) Landslide hazard and risk: concluding comment and perspectives. In: Glade T, Anderson M, Crozier M (eds) Landslide hazard and risk. Wiley, Chichester, pp 767–774

Gomez H, Kavzoğlu T (2005) Assessment of shallow landslide susceptibility using artificial neural networks in Jabonosa River Basin, Venezuela. Eng Geol 78:11–27

Guzzetti F, Ardizzone F, Cardinali M, Galli M, Reichenbach P, Rossi M (2008) Distribution of landslides in the Upper Tiber River basin, central Italy. Geomorphology 96:105–122

Hasekiogullari GD (2010) Assessment of parameter effects in producing landslide susceptibility maps. Hacettepe University Geological Engineering Department, MSc Thesis, Ankara (in Turkish) http://tumas.meteoroloji.gov.tr. Accessed 03 January 2009

Huang PH, Tsai JS, Lin WT (2010) Using multiple-criteria decision-making technique for eco-environmental vulnerability assessment: a case study on the Chi-Jia-Wan Stream watershed, Taiwan. Environ Monit Assess 168:141–158

Kanungo DP, Arora MK, Sarkar S, Gupta RP (2006) A comparative study of conventional, ANN black box, fuzzy and combined neural and fuzzy weighting procedures for landslide susceptibility zonation in Darjeeling Himalayas. Eng Geol 85:347–366

Komac M (2006) A landslide susceptibility model using analytical hierarchy process method and multivariate statistics in perialpine Slovenia. Geomorphology 74:17–28

Lee S, Talib JA (2005) Probabilistic landslide susceptibility and factor effect analysis. Environ Geol 47:982–990

Lee S, Ryu JH, Won JS, Park HJ (2004) Determination and application of the weights for landslide susceptibility mapping using an artificial neural network. Eng Geol 71:289–302

Meusburger K, Alewell C (2008) Impacts of anthropogenic and environmental factors on the occurrence of shallow landslides in an alpine catchment (Urseren Valley, Switzerland). Nat Haz Earth Syst Sci 8:509–520

Moore ID, Wilson JP (1992) Length–slope factors for the revised universal soil loss equation: simplified method for estimation. J Soil Wat Cons 47:423–428

Moore ID, Grayson RB, Ladson AR (1991) Digital terrain modeling: a review of hydrological, geomorphological, and biological applications. Hydro Proc 5:3–30

Moreiras SM (2005) Landslide susceptibility zonation in the Rio Mendoza Valley, Argentina. Geomorphology 66:345–357

MTA (2002) 1/25000 scale geological database (in Turkish)

Nandi A, Shakoor A (2009) A GIS-based landslide susceptibility evaluation using bivariate and multivariate statistical analyses. Eng Geol 110:11–20

Nefeslioglu HA, Duman TY, Durmaz S (2008) Landslide susceptibility mapping for a part of tectonic Kelkit Valley (Eastern Black Sea region of Turkey). Geomorphology 94:401–418

Oh JJ, Pradhan B (2011) Application of a neuro-fuzzy model to landslide susceptibility mapping in a tropical hilly area. Comp Geosci 37(9):1264–1276

Poudyal CP, Chang C, Oh HJ, Lee S (2010) Landslide susceptibility maps comparing frequency ratio and artificial neural networks: a case study from the Nepal Himalaya. Environ Earth Sci 61:1049–1064

Pradhan B (2010a) Landslide susceptibility mapping of a catchment area using frequency ratio, fuzzy logic and multivariate logistic regression approaches. J Ind Soc Rem Sens 38(2):301–320

Pradhan B (2010b) Remote sensing and GIS-based landslide hazard analysis and cross-validation using multivariate logistic regression model on three test areas in Malaysia. Advncs Space Res 45(10):1244–1256

Pradhan B (2010c) Application of an advanced fuzzy logic model for landslide susceptibility analysis. Int J Comp Int Sys 3(3):370–381

Pradhan B (2011) Use of GIS based fuzzy relations and its cross application to produce landslide susceptibility maps in three test areas in Malaysia. Environ Earth Sci 63(2):329–349

Pradhan B, Buchroithner MF (2010) Comparison and validation of landslide susceptibility maps using an artificial neural network model for three test areas in Malaysia. Environ Eng Geosci 2:107–126

Pradhan B, Lee S (2010) Landslide susceptibility assessment and factor effect analysis: backpropagation artificial neural networks and their comparison with frequency ratio and bivariate logistic regression modelling. Environ Model Soft 25:747–759

Pradhan B, Pirasteh P (2010) Comparison between prediction capabilities of neural network and fuzzy logic techniques for landslide susceptibility mapping. Distr Advncs 3(2):26–34

Pradhan B, Lee S, Buchroithner MF (2009) Use of geospatial data and fuzzy algebraic operators to landslide-hazard mapping. Appl Geomat 1:3–15

Pradhan B, Lee S, Buchroithner MF (2010a) Remote sensing and GIS-based landslide susceptibility analysis and its cross-validation in three test areas using a frequency ratio model. Photogramm Fernerkundung Geoinformation 1:17–32

Pradhan B, Sezer E, Gokceoglu C, Buchroithner MF (2010b) Landslide susceptibility mapping by neuro-fuzzy approach in a landslide prone area (Cameron Highland, Malaysia). IEEE Trans Geosci Rem Sens 48(12):4164–4177

Ross TJ (1995) Fuzzy logic with engineering applications. Mc-Graw-Hill, New Mexico

Rouse JW, Haas RH, Deering DW, Schell JA, Harlan JC (1974) Monitoring the vernal advancement and retrogradation (Green Wave Effect) of natural vegetation, NASA/GSFC Type III Final Report, Greenbelt

Ruff M, Czurda K (2008) Landslide susceptibility analysis with a heuristic approach in the Eastern Alps (Vorarlberg, Austria). Geomorphology 94:314–324

Saaty TL (1977) A scaling method for priorities in hierarchical structures. J Math Psychol 15:234–281

Saaty TL, Vargas GL (2001) Models, methods, concepts and applications of the analytic hierarchy process. Kluwer, Boston

Sezer E, Pradhan B, Gokceoglu C (2011) Manifestation of an adaptive neuro-fuzzy model on landslide susceptibility mapping: Klang valley, Malaysia. Exp Systms App 38(7):8208–8219

Soeters R, Van Westen CJ (1996) Slope instability recognition, analysis and zonation. In: Turner AK, Schuster R (eds) Landslides investigation and mitigation. Transportation Research Board Special report, 247. National Academy Press, Washington
Strahler AN (1957) Quantitative analysis of watershed geomorphology. Trans Am Geophys Union 38:913–920
Thiery Y, Malet JP, Sterlacchini S, Puissant A, Maquaire O (2007) Landslide susceptibility assessment by bivariate methods at large scales: application to a complex mountainous environment. Geomorphology 92:38–59
Tuysuz O, Aksay A, Yiğitbaş E (2004) Batı Karadeniz Bölgesi litostratigrafi birimleri. Stratigrafi Komitesi litostratigrafi birimleri serisi-1. MTA Genel Müdürlüğü Eğitim Serisi, Ankara (in Turkish)
Van Westen CJ (2000) The modelling of landslide hazards using GIS. Surv Geophys 21:241–255
Van Westen CJ, Castellanos E, Kuriakose SL (2008) Spatial data for landslide susceptibility, hazard, and vulnerability assessment: an overview. Eng Geol 102:112–131
Wang WD, Xie CM, Du XG (2009) Landslides susceptibility mapping based on geographical information system, GuiZhou, south-west China. Environ Geol 58:33–43
Yalçın A (2008) GIS-based landslide susceptibility mapping using analytical hierarchy process and bivariate statistics in Ardesen (Turkey): comparisons of results and confirmations. Catena 72:1–12
Yalçın A, Bulut F (2007) Landslide susceptibility mapping using GIS and digital photogrammetric techniques: a case study from Ardesen (NE-Turkey). Nat Haz 41:201–226
Yeşilnacar E, Topal T (2005) Landslide susceptibility mapping: a comparison of logistic regression and neural networks methods in a medium scale study, Hendek region (Turkey). Eng Geol 79:251–266
Yılmaz I (2009) Landslide susceptibility mapping using frequency ratio, logistic regression, artificial neural networks and their comparison: a case study from Kat landslides (Tokat-Turkey). Comp Geosci 35(6):1125–1138
Yılmaz I (2010) Comparison of landslide susceptibility mapping methodologies for Koyulhisar, Turkey: conditional probability, logistic regression, artificial neural networks, and support vector machine. Environ Earth Sci 61:821–836